Stark broadening of hydrogenic heavy ions in dense inertial-confinement fusion plasmas

B. Held
Laboratoire d'Electricité, Université de Pau, Avenue Philippon, F-64000 Pau, France

C. Deutsch and M.-M. Gombert
Laboratoire de Physique des Plasmas (Laboratoire associé au Centre National de la Recherche Scientifique), Bâtiment 212, Université de Paris XI, F-91405 Orsay Cedex, France

(Received 31 May 1983)

The low-frequency microfield distributions obtained for dense ionic mixtures are used to compute the complete combined Stark and Doppler profiles of Lyman α and β lines emitted by Ne X and Ar XVIII immersed in dense proton plasmas of interest for inertial-confinement fusion (ICF). Electron broadening is treated within the impact approximation. A certain emphasis is paid to the ion proportion effect, conveniently analyzed through $p=C_b/(C_b+C_a)$. A novel feature of the present calculation is afforded by the wings' behavior that is fully investigated analytically. For $|\Delta\nu|\geq 2$ Ry, the asymptotic profiles fall within 1% of the completely numerical ones (Doppler excluded). Excellent agreement with previous Tighe-Hooper calculations is achieved. Extensive numerical results are given for V up to 0.8 (where the spectroscopy parameter V is r_0/λ_{D_e}, the ratio between the classical radius of the electron and the electron Debye length).

I. INTRODUCTION

There is always an important demand for accurate spectroscopic data for the diagnostic of dense and host plasmas produced in order to achieve inertial-confinement fusion (ICF).[1] These beam—or laser—created plasmas may be analyzed in the best nondestructive way through the line broadening of high Z and highly stripped hydrogenic species immersed on purpose, in the dense and hot proton fluid of ICF interest.[1,2]

A large amount of theoretical effort has already been devoted to the computation of hydrogenic Stark profiles.[3] The present work takes advantage of the accurate and efficient numerical code displayed in the preceding paper[4] to compute rapidly the low-frequency electric microfield in a binary ionic mixture of ions a and b with any proportion $p=C_b/(C_a+C_b)$.

The low-frequency microfield is an essential ingredient of a complete profile calculation,[5,6] which has to be recalculated for each emitter charge. In this context, we have been able to check out that the Baranger-Mozer[7] (BM) cluster expansion, when improved numerically, can reproduce the cold plasmas[9] data obtained by Hooper within 0.5%.

Fortunately, it turns out that the BM approach is even more flexible and still as accurate for low-frequency microfield data at highly stripped ions in dense plasmas of ICF interest with typically[4] $10^{22}\leq n_e\leq 10^{24}$ $e\,\mathrm{cm}^{-3}$ and $10^6\leq T_e\leq 10^7$ K. Extrapolating somewhat from the present ICF diagnostics[1,2] needs mostly based on laser compressed plasmas, we do consider also dense mixtures of heavy ions in any relative proportions in relation to the multishells target planned for heavy ions driven fusion.[11,12]

In this area, up to now, the main emphasis has been laid on the line center around $|\Delta\nu|\leq 0.8$ Ry, where the broadening results from a strong interplay between electron impact, statistical Doppler, and quasistatic ion contributions. Moreover, we think it useful to also investigate the wings beyond 0.8 Ry, which are now accessible to experimental verifications[2,13] in dense plasma conditions.

For this purpose we make use of the asymptotic $H(\beta)$ developed in Ref. 4 for $\beta\geq 5$, altogether with an analytic electron collision operator for the Lyman series, to obtain accurate asymptotic wings formulas. The basic impact formalism[5,6] for Ly α and β emitted by highly stripped heavy ions is developed in Sec. II.

The line center results ($|\Delta\nu|\leq 0.8$ Ry) are discussed at length in Sec. III for ionic mixtures with any proportions. The wings treatment is detailed in Sec. IV.

II. BASIC THEORY

A. General

The complete line calculations are based on the now standard generalized impact theory[5,6] making use of complete electron-atom collisions for the electron Stark broadening. The electron fluid is taken as nondegenerate. Actually, even in rather extreme conditions such as

$$n_e\sim 10^{24}\ e\,\mathrm{cm}^{-3}$$

and

$$T_e\cong 1.26\times 10^6\ \mathrm{K}\ ,$$

the classical electron plasma parameter[9] $\Lambda_e=\beta e^2/\lambda_{D_e}\cong 0.171$ and the degeneracy parameter

$\chi=(\ln 2)^{5/2}\pi^3 n_e \lambdabar_{ee}^3 \cong 0.042$, with n_e in cm^{-3}, provide ample support for a classical treatment of the electronic component.

In practice, we shall be restricted to smaller densities and comparable or higher temperatures. Adapting the neutral atom Lyman formalism[6] to hydrogen lines emitted by heavy ions retaining one electron, one is led to consider the impact electron profile[5]

$$I_{\vec{e}}^{S}(\omega,\vec{\mathrm{E}})=\frac{1}{\pi}R_e \sum_{i,j,k} \langle \psi_i \mid \vec{\mathrm{e}}\cdot\vec{\mathrm{r}} \mid \phi_j \rangle \langle \phi_j \mid \vec{\mathrm{e}}\cdot\vec{\mathrm{r}} \mid \psi_k \rangle \times \langle \psi_k \mid [i(\Delta\omega-\Delta\omega_i)-\Phi^{(n)}]^{-1} \mid \psi_i \rangle \; . \tag{1}$$

ψ_i and ψ_k denote the upper-level n wave functions. ϕ_j is the nondegenerate ground state. $\phi^{(n)}$ is the electron collision operator acting on the upper level. We may safely neglect any collision broadening of the ground state.

The frequency shift $\Delta\omega=\omega-\omega_0$ is counted from the unperturbed line

$$\omega_0=\frac{E_0^{(n)}-E_0^{(n')}}{\hbar}=\frac{Z_N^2 e^2}{2a_0\hbar}\left[\frac{1}{n'^2}-\frac{1}{n^2}\right],$$

where Z_N is the emitter nuclear charge and a_0 the Bohr radius. In Eq. (1)

$$\Delta\omega_i=\hbar^{-1}\langle \psi_i \mid (H-E_0^{(n)}) \mid \psi_i \rangle \; .$$

Taking the electric field $\vec{\mathrm{E}}$ along Oz, the static properties are easily deduced from the Schrödinger problem

$$H \mid \psi_i \rangle = E^{(n)} \mid \psi_i \rangle \tag{2}$$

with

$$H=H_0+ezE \; ,$$

$$H_0=\frac{p^2}{2m_e}-Z_N\frac{e^2}{r} \; .$$

$\Delta\omega_i$ is thus deduced from ($A=eaE$)

$$(Az/a_0)\mid \psi_i \rangle = \xi_i \mid \psi_i \rangle \tag{3}$$

through

$$\Delta\omega_i=\xi_i/\hbar \; .$$

The emitted profile is thus normalized by setting

$$\vec{\mathrm{R}}=\frac{\vec{\mathrm{r}}}{a_0}\frac{1}{[I(n',n)]^{1/2}} \; , \tag{4}$$

in terms of the whole line intensity

$$I(n',n)=\tfrac{1}{3}\sum_l (l+1)(R_{nl}^{n',l+1})^2+l(R_{nl}^{n',l-1})^2 \; , \tag{5}$$

where $R_{nl}^{n',l\pm 1}$ are the usual hydrogenic radial integrals[14] $\int_0^\infty dr\, r^2 R_{nl}(r)R_{n'l\pm 1}(r)$ involved in dipolar matrix elements. Equation (1) is then detailed through the expansions

$$\mid \psi_i \rangle = \sum_{p=1}^{n^2} a_i^p \mid n,p \rangle \; , \qquad \mid \phi_b \rangle = \sum_{r=1}^{n'^2} b_j^r \mid n',r \rangle \tag{6}$$

in terms of the spherical hydrogenic states $\mid n,l,m \rangle$ (here denoted as $\mid n,p \rangle$) with $p=l(l+1)+m+1$.

The corresponding normalized electron profile thus reads

$$S_{\vec{e}}^{S}(\omega,E)=\frac{1}{\pi}\sum_{i=1}^{n^2}\sum_p I_{i\vec{e}}^{p}\frac{\phi_p^{(n)}}{(\phi_p^{(n)})^2+(\Delta\omega-\Delta\omega_i)^2} \; , \tag{7}$$

where

$$I_{i\vec{e}}^{p}=a_i^p\sum_q a_i^q \langle nq \mid \vec{\mathrm{e}}\cdot\vec{\mathrm{R}} \mid 1 \rangle \langle 1 \mid \vec{\mathrm{e}}\cdot\vec{\mathrm{R}} \mid np \rangle \; .$$

The complete Stark profile including the low-frequency averaging is then ($\omega=2\pi\nu$)

$$S_{\vec{e}}^{S}(\nu)=\int_0^\infty S_{\vec{e}}^{S}(\nu,\beta)H(\beta)d\beta \; . \tag{8}$$

The statistical Doppler effect is finally included through the folding

$$S(\nu)=\int_{-\infty}^{+\infty} S^D(\nu-\nu')S^S(\nu')d\nu' \; , \tag{9}$$

where

$$S^D(\nu-\nu')=\frac{Mc^2}{2\pi k_B T}\exp\left[-\frac{Mc^2}{2k_B T}\left[\frac{\nu-\nu'}{\nu_0}\right]^2\right] . \tag{10}$$

M is the ionic mass and $\nu_0=Z_N^2(1/n'^2-1/n^2)$ Ry.

First, the statically perturbed ionic parameters are deduced from the eigenvalue problem

$$\sum_{p=1}^{n^2}\left[A\frac{z}{a_0}-\xi_i\right]a_i^p \mid n,p \rangle = 0 \; . \tag{11}$$

On the other hand, the electron collision operator

$$\phi^{(n)}=\frac{4\pi n_e}{3}\left[\frac{8k_B T}{\pi m_e}\right]^{1/2}\bar{\rho}^2 D \; , \tag{12}$$

where

$$\bar{\rho}^2=\left[\frac{\hbar}{m_e}\right]^2\frac{m_e}{2k_B T_e}\left\langle\frac{\vec{\mathrm{r}}\cdot\vec{\mathrm{r}}}{a_0^2}\right\rangle ,$$

$$D=\ln\left[\frac{\lambda_{De}}{\langle r \rangle}\right]$$

is explained through

$$\left\langle\frac{\vec{\mathrm{r}}\cdot\vec{\mathrm{r}}}{a_0^2}\right\rangle=\left\langle n,l,m\left|\frac{\vec{\mathrm{r}}\cdot\vec{\mathrm{r}}}{a_0^2}\right|n,l,m\right\rangle =\frac{9}{4}\frac{n^2}{Z_N^2}[n^2-(l^2+l+1)] \; , \tag{13}$$

$$\langle r \rangle = (\langle n,l,m \mid r^2 \mid n,l,m \rangle)^{1/2} =\frac{na_0}{\sqrt{2}Z_N}[5n^2+1-3l(l+1)]^{1/2}$$

under the form

$$\frac{\phi^{(n)}}{2\pi}=\frac{1.25\times10^{-21}}{Z_N^2}\frac{n_e}{T_e^{1/2}}n^2[n^2-(l^2+l+1)]\times\left\{21.33-\ln\{n[5n^2+1-3l(l+1)]^{1/2}\}-\ln\left[\frac{1}{Z_N}\left[\frac{n_e}{T_e}\right]^{1/2}\right]\right\}, \tag{14}$$

in Ry, with n_e in cm^{-3} and T_e in K.

B. Ly α

Equation (11) is now specialized as

$$\begin{bmatrix} -\xi & 0 & \frac{3A}{Z_N} & 0 \\ 0 & -\xi & 0 & 0 \\ \frac{3A}{Z_N} & 0 & -\xi & 0 \\ 0 & 0 & 0 & -\xi \end{bmatrix}\begin{bmatrix} a^1 \\ a^2 \\ a^3 \\ a^4 \end{bmatrix}=0, \tag{15}$$

through a characteristic equation

$$\xi^2\left[\xi^2-9\frac{A^2}{Z_N^2}\right]=0$$

with eigenvalues

$$\xi_1=0,$$
$$\xi_2=0,$$
$$\xi_3=\frac{3A}{Z_N},$$
$$\xi_4=-\frac{3A}{Z_N},$$

and eigenkets $a^2=a^4=0$,

$$a^1=-\frac{\xi}{(\xi^2+9A^2/Z_N^2)^{1/2}},$$
$$a^3=-\frac{\xi}{(\xi^2+9A^2/Z_N^2)^{1/2}}.$$

Dipolar selection rules[14] immediately yield

$$S_{Ox}^S=S_{Oy}^S=0, \tag{16}$$
$$S_{Oz}^S=\frac{1}{\pi}\sum_{i=1}^{4}\left[\frac{a_i^3}{Z_N}\right]^2\frac{\phi_3^{(2)}}{(\phi_3^{(2)})^2+(\Delta\omega-\Delta\omega_i)^2},$$

where, with n_e in cm^{-3} and T_e in K,

$$\frac{\phi_3^{(2)}}{2\pi}=5.00\times10^{-21}\left\{19.28-\ln\left[\frac{1}{Z_N}\left[\frac{n_e}{T_e}\right]^{1/2}\right]\right\}\times\frac{1}{Z_N^2}\frac{n_e}{T_e^{1/2}}, \tag{17}$$

and

$$n=2 \text{ and } p=3\ (l=1,\ m=0),$$

so that

$$S_{Oz}^S=\frac{1}{2\pi}\frac{1}{Z_N^2}\frac{1}{\phi_3^{(2)}}\left\{4\left[1+\left[\frac{\Delta\nu}{\phi_3^{(2)}/2\pi}\right]^2\right]^{-1}+\left[1+\left[\frac{\Delta\nu+C^{(2)}\beta}{\phi_3^{(2)}/2\pi}\right]^2\right]^{-1}+\left[1+\left[\frac{\Delta\nu-C^{(2)}}{\phi_3^{(2)}/2\pi}\right]^2\right]^{-1}\right\} \tag{18}$$

with $C^{(2)}=4.37\times10^{-16}(n_e^{2/3}/Z_N)$, where n_e is in cm^{-3} and $C^{(2)}$ in Ry.

C. Ly β

Equation (11) now becomes

$$\begin{bmatrix}
-\xi & 0 & 3\sqrt{6}\frac{A}{Z_N} & 0 & 0 & 0 & 0 & 0 & 0 \\
0 & -\xi & 0 & 0 & 0 & \frac{9}{2}\frac{A}{Z_N} & 0 & 0 & 0 \\
3\sqrt{6}\frac{A}{Z_N} & 0 & -\xi & 0 & 0 & 0 & 3\sqrt{3}\frac{A}{Z_N} & 0 & 0 \\
0 & 0 & 0 & -\xi & 0 & 0 & 0 & \frac{9}{2}\frac{A}{Z_N} & 0 \\
0 & 0 & 0 & 0 & -\xi & 0 & 0 & 0 & 0 \\
0 & \frac{9}{2}\frac{A}{Z_N} & 0 & 0 & 0 & -\xi & 0 & 0 & 0 \\
0 & 0 & 3\sqrt{3}\frac{A}{Z_N} & 0 & 0 & 0 & -\xi & 0 & 0 \\
0 & 0 & 0 & \frac{9}{2}\frac{A}{Z_N} & 0 & 0 & 0 & -\xi & 0 \\
0 & 0 & 0 & 0 & 0 & 0 & 0 & 0 & -\xi
\end{bmatrix}\begin{bmatrix} a^1 \\ a^2 \\ a^3 \\ a^4 \\ a^5 \\ a^6 \\ a^7 \\ a^8 \\ a^9 \end{bmatrix}=0 \tag{19}$$

with

$$\xi^3(\xi^2-\tfrac{81}{4}A^2/Z_N^2)^2(\xi^2-81A^2/Z_N^2)=0 ,$$

so that

$$\xi_1=\xi_2=\xi_3=0 ,$$
$$\xi_4=\frac{9}{2}\frac{A}{Z_N} ,$$
$$\xi_5=-\frac{9}{2}\frac{A}{Z_N} ,$$
$$\xi_6=\frac{9}{2}\frac{A}{Z_N} ,$$
$$\xi_7=-\frac{9}{2}\frac{A}{Z_N} ,$$
$$\xi_8=9\frac{A}{Z_N} ,$$
$$\xi_9=-9\frac{A}{Z_N} ,$$

and $a^2=a^4=a^5=a^6=a^8=a^9=0$,

$$a^1=\frac{(\xi^2-27A^2/Z_N^2)}{(\xi^4+2187A^4/Z_N^4)^{1/2}} ,$$
$$a^3=\frac{3\sqrt{6}A/Z_N}{(\xi^4+2187A^4/Z_N^4)^{1/2}} ,$$
$$a^7=\frac{27\sqrt{2}A^2/Z_N^2}{(\xi^4+2187A^4/Z_N^4)^{1/2}} .$$

Again the dipole selection rules impose

$$S_{Ox}^S=S_{Oy}^S=0 ,$$
$$S_{Oz}^S=\frac{1}{\pi}\sum_{i=1}^{9}\left[\frac{a_i^3}{Z_N}\right]^2\frac{\phi_3^{(3)}}{(\phi_3^{(3)})^2+(\Delta\omega-\Delta\omega_i)^2} , \tag{20}$$

where

$$\frac{\phi_3^{(3)}}{2\pi}=6.76\times10^{-20}\left\{18.39-\ln\left[\frac{1}{Z_N}\left[\frac{n_e}{T_e}\right]^{1/2}\right]\right\}\times\frac{1}{Z_N^2}\frac{n_e}{T_e^{1/2}} ,$$

with n_e in cm^{-3} and T_e in K. The nonzero electron profile thus reads

$$S_{Oz}^S=\frac{1}{2\pi}\frac{1}{Z_N^2}\frac{1}{\Phi_3^{(3)}}\left\{\frac{32}{19}\left[1+\left[\frac{\Delta\nu+C^{(3)}\beta}{\Phi_3^{(3)}/2\pi}\right]^2\right]^{-1}+\frac{32}{19}\left[1+\left[\frac{\Delta\nu-C^{(3)}\beta}{\Phi_3^{(3)}/2\pi}\right]^2\right]^{-1}+\left[1+\left[\frac{\Delta\nu+2C^{(3)}}{\Phi_3^{(3)}/2\pi}\right]^2\right]^{-1}+\left[1+\left[\frac{\Delta\nu-2C^{(3)}\beta}{\Phi_3^{(3)}/2\pi}\right]^2\right]^{-1}\right\} \tag{21}$$

with $C^{(3)}=6.56\times10^{-16}(n_e^{2/3}/Z_N)$ Ry, where n_e is in cm^{-3}.

III. NUMERICAL PROFILES (LINE CENTER)

A. Heavy ions impurities in dense protons $[p=C_b/(C_a+C_b)\cong1]$

For obvious ICF purposes, we pay particular attention to Stark + Doppler profiles emitted by hydrogenic Ne X and Ar XVIII impurities denoted as a, and immersed in dense and hot protons (denoted as b). The corresponding n_e and T_e values are selected out so that the relevant spectroscopic parameter, with n_e in cm^{-3},

$$V=\frac{r_0}{\lambda_{D_e}}=\frac{8.98\times10^{-2}n_e^{1/6}}{T_e^{1/2}} , \tag{22}$$

index the low-frequency microfield $H(\beta)$ data displayed in Ref. 4.

The emitted intensities are plotted in relative unit I/I_0, where I_0 denotes the right-hand side (rhs) of Eq. (5). When available, we retrieve the precious Tighe-Hooper (TH) results[3] for Ly α within 0.5% except in the very center ($\Delta\nu\leq0.05$ Ry) where our results could exhibit some discrepancies because of the impact treatment[5,6] for electron collision broadening.

The TH approach makes use of a relaxation approximation which allows for incomplete electron-atom encounters. However, we do not think such a discrepancy is a really significant one because of a likely reabsorption in the vicinity of the center of the resonance transitions considered presently. Figures 1 and 4 for Ar XVIII and Ne X, respectively, demonstrate the importance of the statistical Doppler broadening. As already pointed out in TH,[3] it is the larger for the heavier ion with the largest Z_N. Figures 2 and 3 contrast a T_e dependence (at fixed n_e) with an n_e dependence (at fixed T_e). As expected,[3] the latter spread is the larger. Such an effect gets even amplified in the Ne X case (Figs. 5 and 6).

As far as a comparison with TH (Ref. 3) is considered, our present calculations extend their calculations beyond $V=0.4$, up to $V=0.8$, i.e., to much more dense compressed plasmas. Similar results are also displayed by the Ly β lines (Figs. 7–12). The dip at $\Delta\nu=0$ allows for a nearly complete removal of the discrepancies with respect to the TH calculations[3] (Figs. 7 and 10). The T_e spread (at fixed n_e) is larger (Fig. 8 versus Fig. 5) than for Ly α.

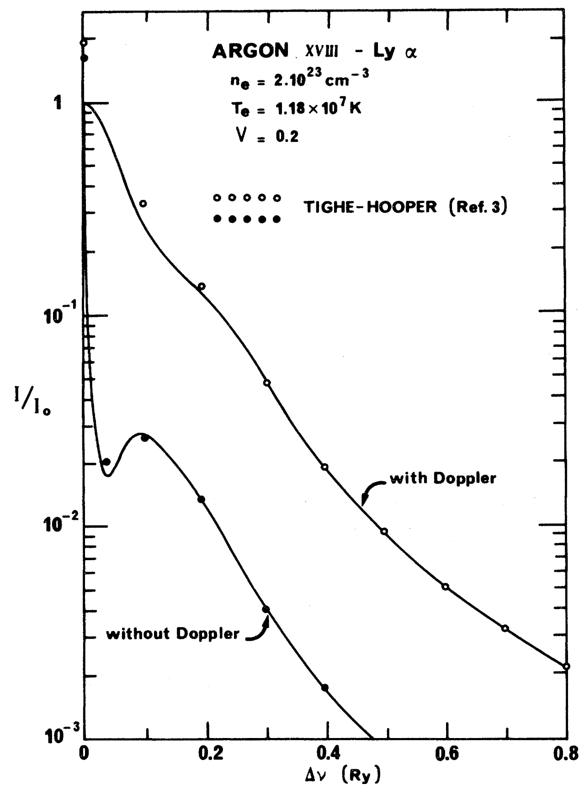

FIG. 1. Ly α profiles emitted by Ar XVIII and Ne X.

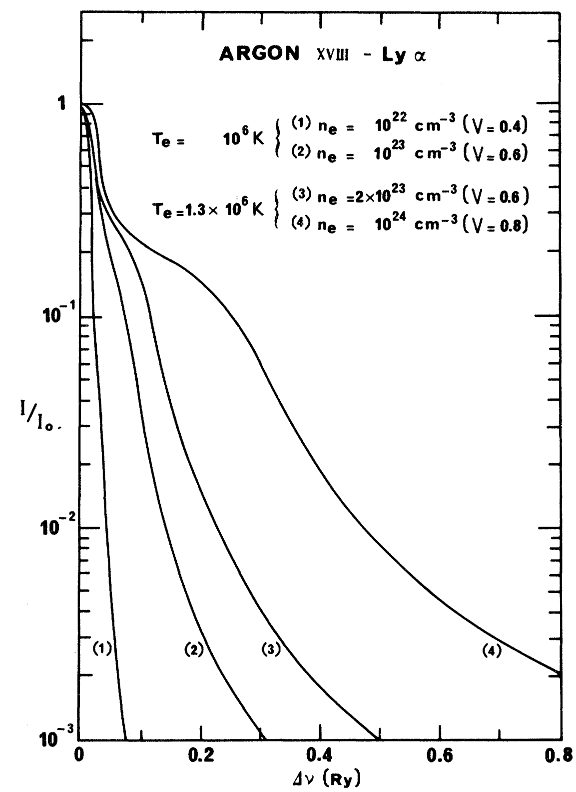

FIG. 3. Ly α profiles emitted by Ar XVIII and Ne X.

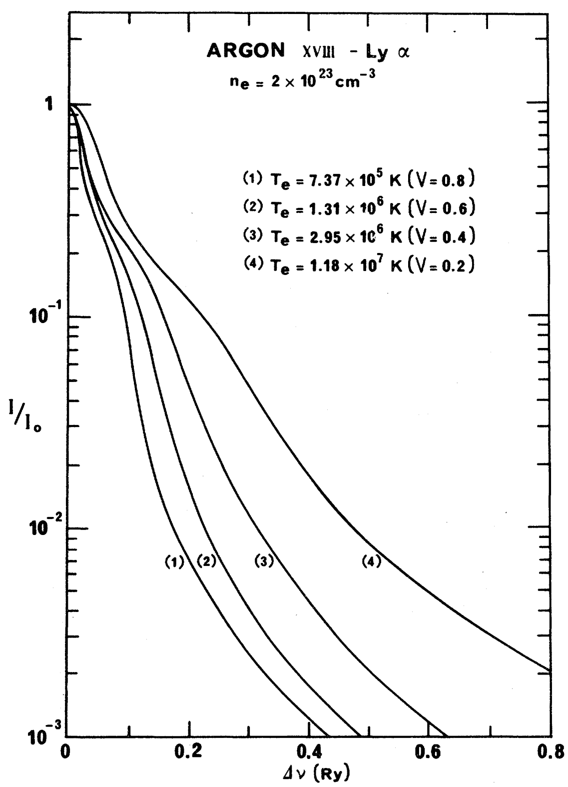

FIG. 2. Ly α profiles emitted by Ar XVIII and Ne X.

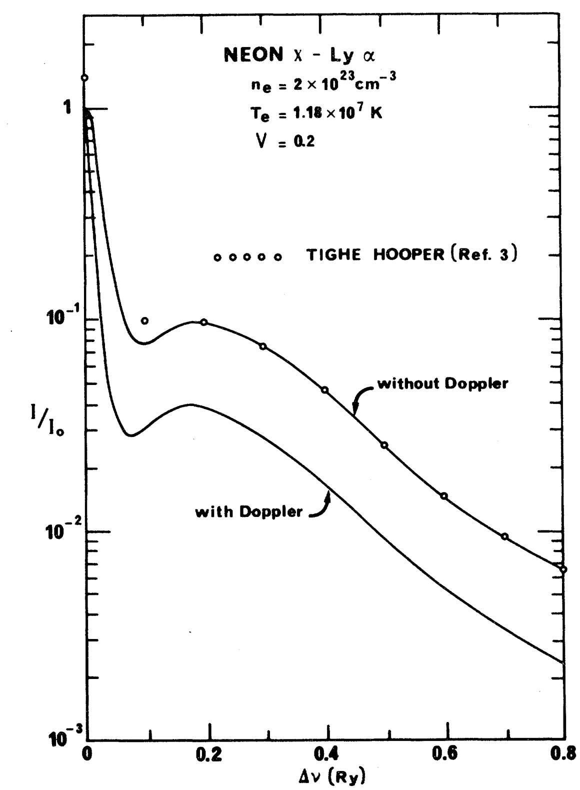

FIG. 4. Ly α profiles emitted by Ar XVIII and Ne X.

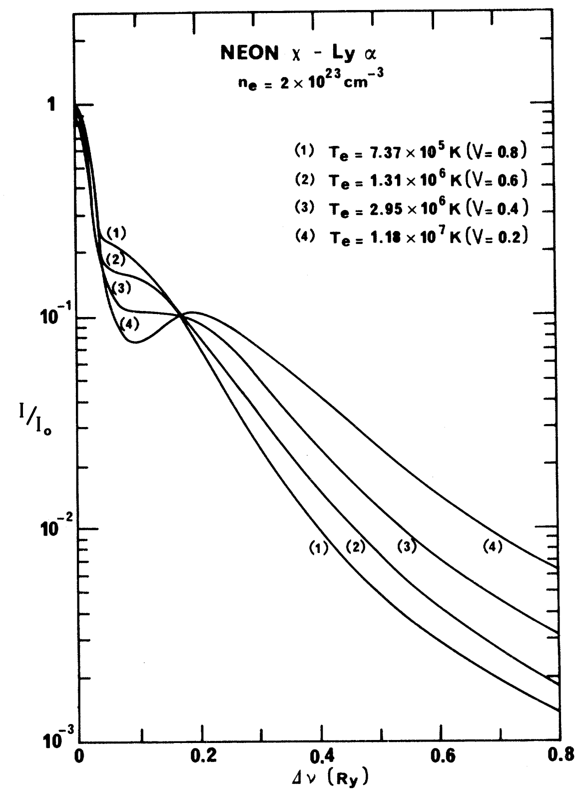

FIG. 5. Ly α profiles emitted by Ar XVIII and Ne X.

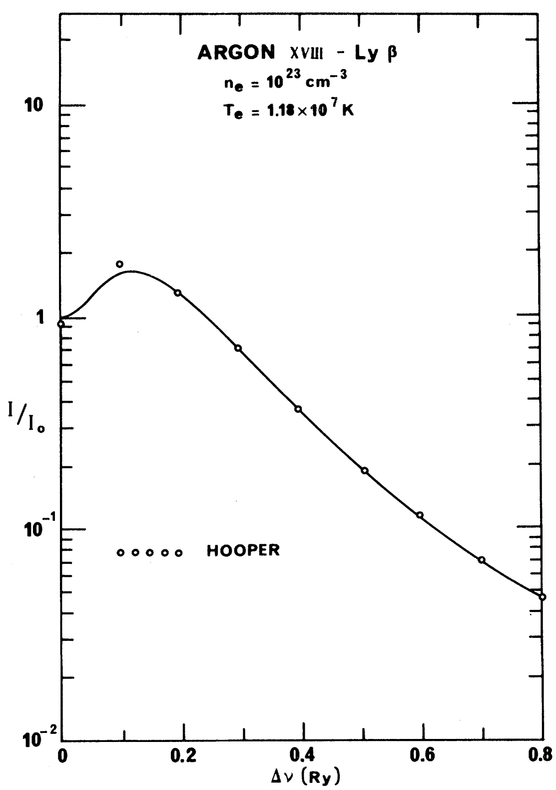

FIG. 7. Ly β profiles emitted by Ar XVIII and Ne X.

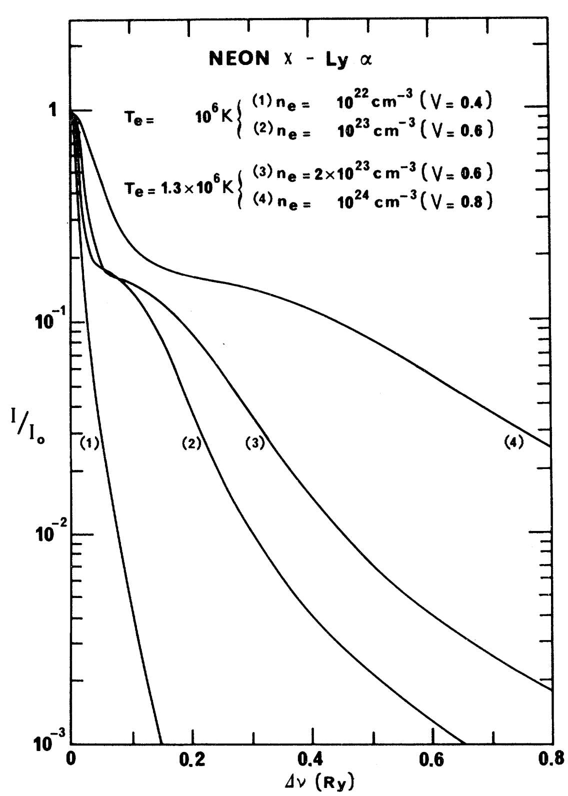

FIG. 6. Ly α profiles emitted by Ar XVIII and Ne X.

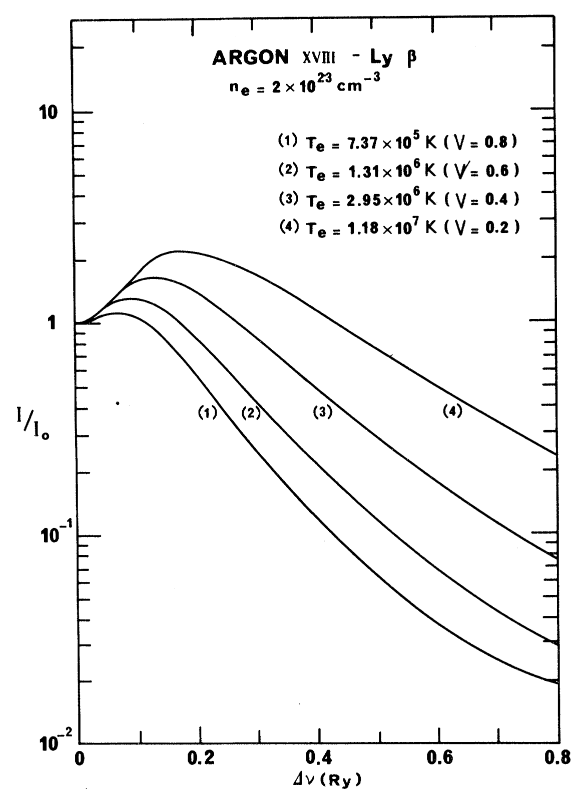

FIG. 8. Ly β profiles emitted by Ar XVIII and Ne X.

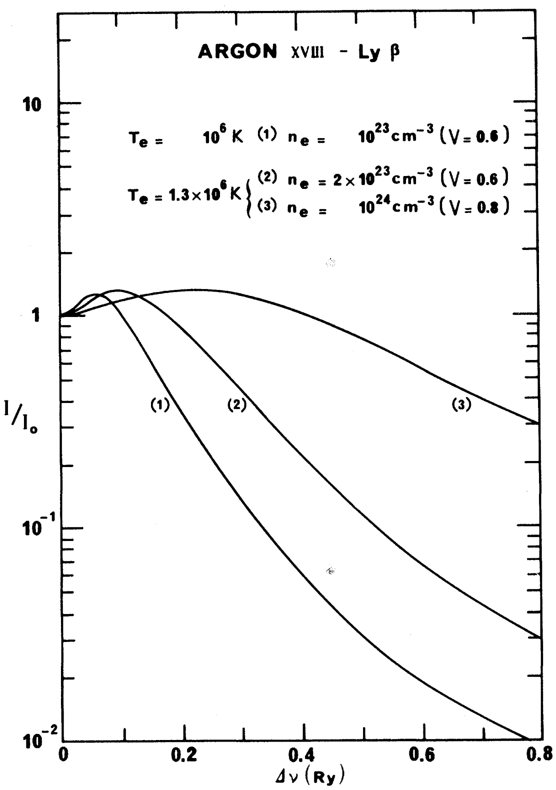

FIG. 9. Ly β profiles emitted by Ar XVIII and Ne X.

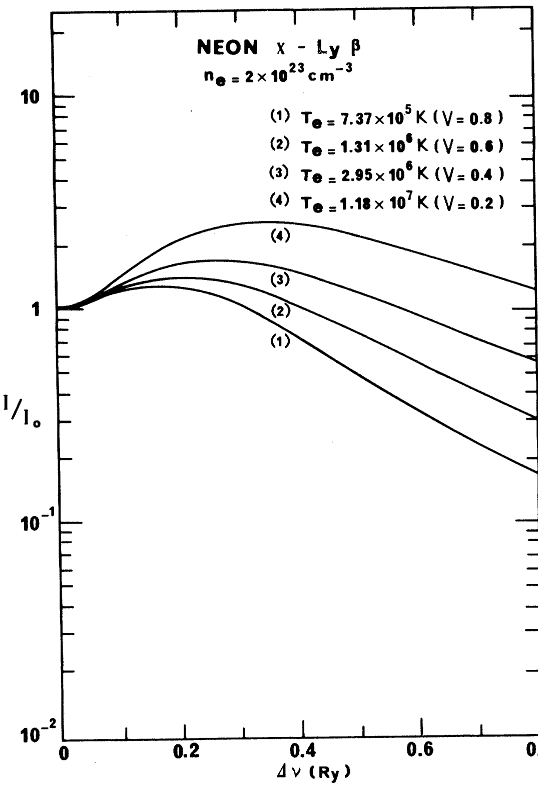

FIG. 11. Ly β profiles emitted by Ar XVIII and Ne X.

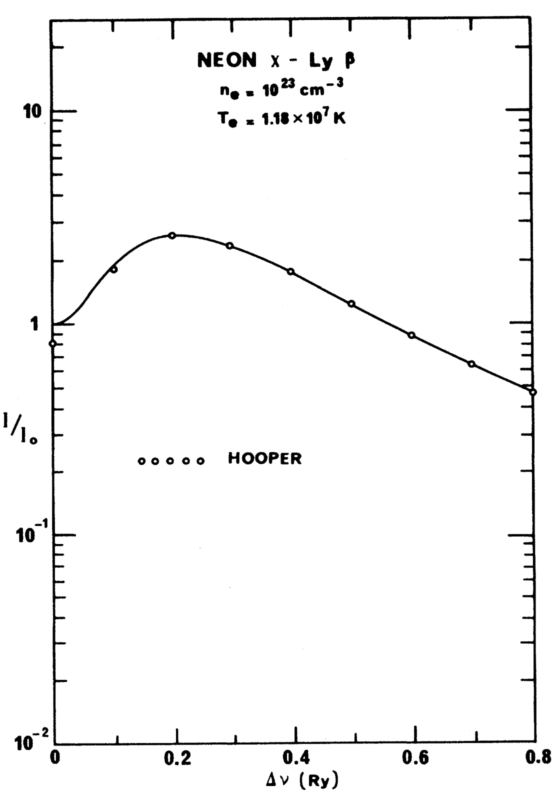

FIG. 10. Ly β profiles emitted by Ar XVIII and Ne X.

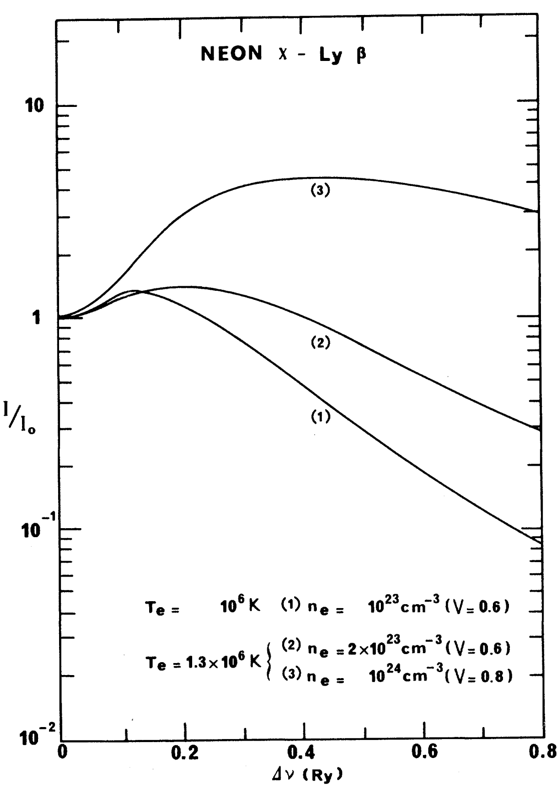

FIG. 12. Ly β profiles emitted by Ar XVIII and Ne X.

B. Proportions effects (any p)

As already mentioned in the Introduction, switching from laser to particle drivers may lead to consider multilayered targets with different heavy ion species in arbitrary relative proportions. For instance, the HIBALL target[11] consists essentially of an outer tamper in Pb, followed by a PbLi pusher in front of the usual D + T fuel.

Therefore, one has to pay attention to proportion effects for any $p=C_b/(C_a+C_b)$ in dense ICF plasmas which could also display strong static correlations measured by the dimensionless classical parameter

$$\Lambda=\frac{\left[1+\dfrac{Z_a^2+p(Z_b^2-Z_a^2)}{Z_a+p(Z_b-Z_a)}\right]^{3/2}}{\left[1+\dfrac{1}{Z_a+p(Z_b-Z_a)}\right]}\Lambda_e \tag{23}$$

with

$$\Lambda_e=\frac{2(2\pi)^{1/2}}{15}V^3=3.34\times10^{-1}V^3 \ .$$

Equation (23) shows clearly that p and Λ effects are interdependent. This contradicts a statement made in Ref. 3 about the negligibility of proportion effects for $v>0.2$. Also, we feel that the parameter $p=C_b/(C_a+C_b)$ is more suitable than $R=n_b/n_a$ to parametrize the proportion effects. Our findings systematize and extend up to $V=0.8$ in the strong correlation regime (Figs. 13 and 14) a general trend already observed qualitatively in Ref. 3, about the very weak p dependence of the emitted profiles in the $0\leq p\leq 0.5$ range. It takes a large proportion of protons (p particles) to counterbalance even a few percent of heavy ions.

It is also worthwhile to notice that the p dependence of the profiles discloses a very transparent onset for the quasistatic Stark broadening through $H(\beta)$. All Ly α profiles merge for $\Delta\nu$ smaller than 0.05 Ry (Figs. 15 and 13) while the Ly β ones (Figs. 16 and 14) split up only around 0.2 Ry. It is quite gratifying that our calculations reproduce fairly well for $\Delta\nu\geq 0.25$ Ry, the Ne X Lyman-β line measured by (Fig. 17) Ya'akobi *et al.*[2]. The discrepancy is likely to arise from optical thickness of the given plasma, in the line center.

IV. WINGS FORMULAS ($\Delta\nu\geq 0.8$ Ry)

Up to now[3] no serious attention has yet been paid to the far wings domain ($\Delta\nu>0.8$ Ry). However, it is now likely that this range may be included within experimental measurements.[13,2] in plasmas with $n_e\sim10^{20}$ $e\,\mathrm{cm}^{-3}$ and $0.5\leq k_BT_e\leq 1$ keV.

Moreover, the analytic nearest-neighbor approximation developed in Ref. 4 for $H(\beta)$, together with the analytic collision operator available in Sec. II, could allow for an easy calculation of accurate wings formulas. However,

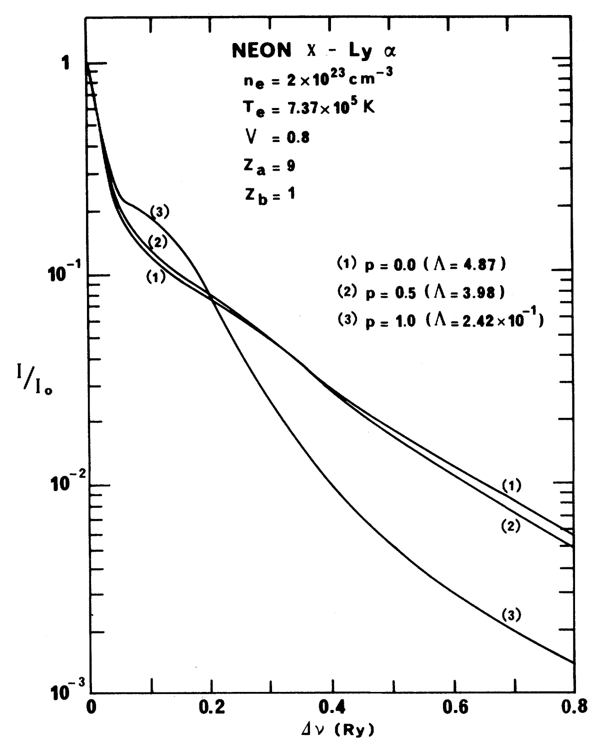

FIG. 13. Proportion effect in strongly correlated plasmas ($V=0.8$).

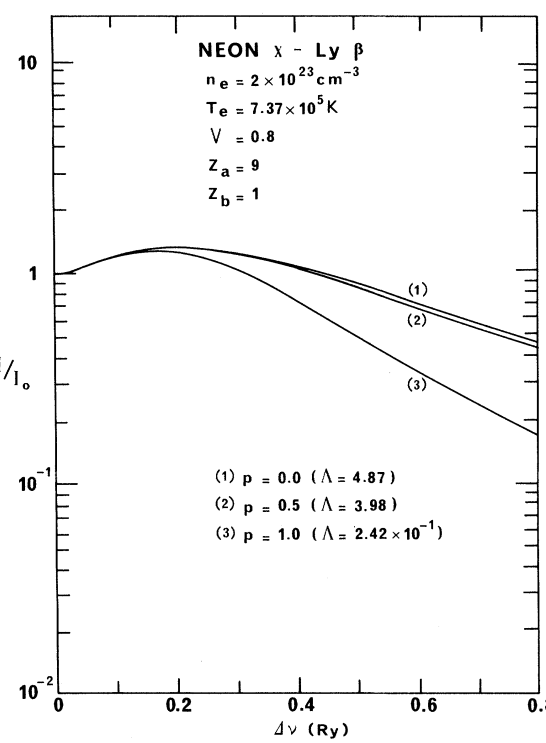

FIG. 14. Proportion effect in strongly correlated plasmas ($V=0.8$).

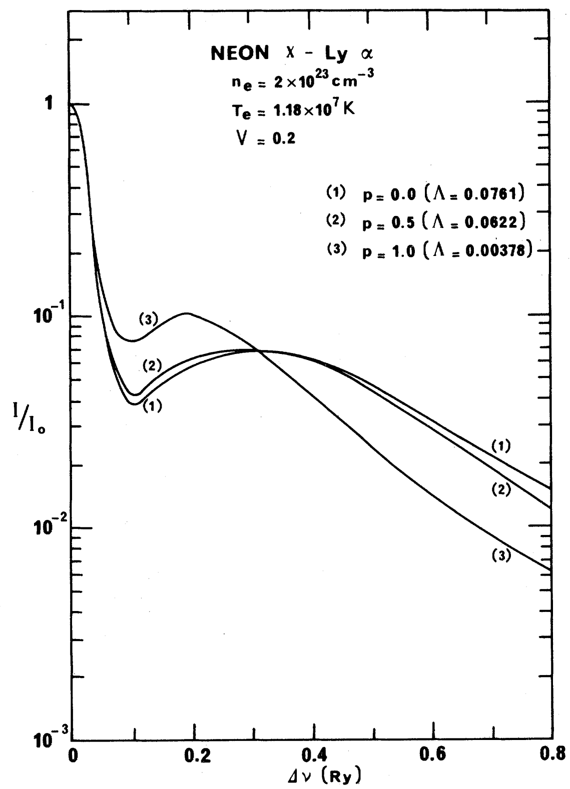

FIG. 15. Ly α profiles emitted by Ar XVIII and Ne X.

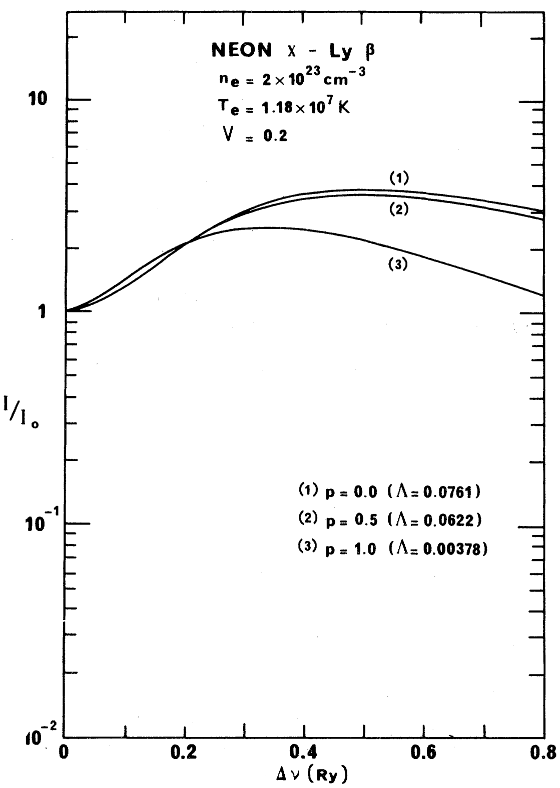

FIG. 16. Ly β profiles emitted by Ar XVIII and Ne X.

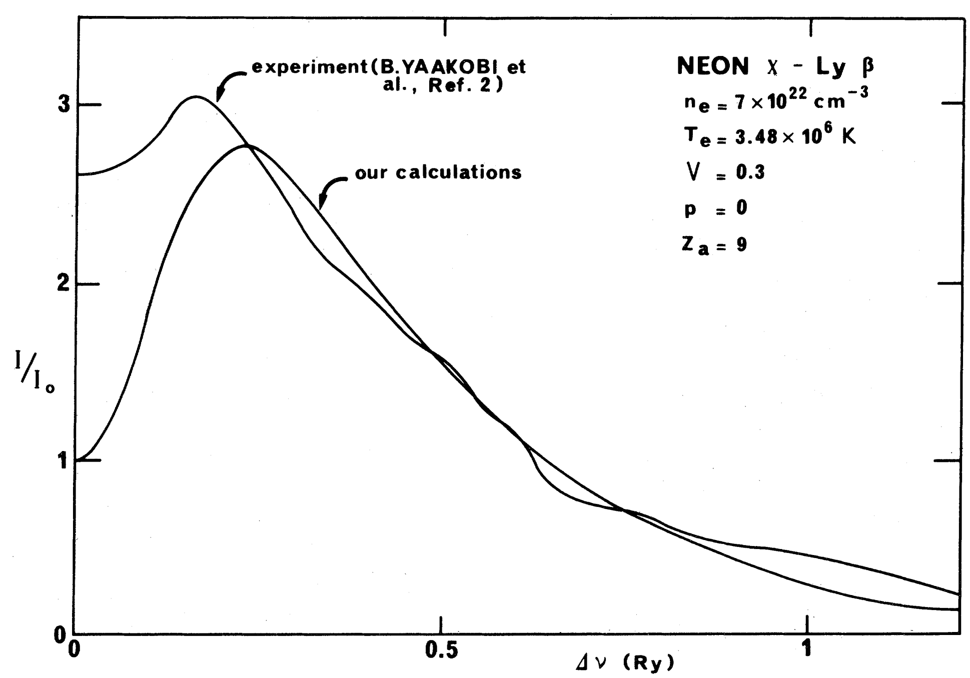

FIG. 17. Computed Ne X Ly β line compared with the experimental results of Ya'akobi *et al.* (Ref. 2).

there is a serious pitfall to avoid. It is due to the ratio $\phi^{(n)}/\Delta\omega$ which becomes smaller than unity, at a critical frequency depending strongly on the line shape and the plasmas conditions.

A. Ly α

Starting with the nonzero electron profile S_{Oz}^{S} (Eq. 18), one can immediately write down

$$\begin{aligned} I(\nu,\beta) &= (2\pi Z_N^2)CS_{Oz}^S \\ &= \frac{4}{1+K^2}+\frac{1}{1+K^2(1+D\beta/\Delta\nu)^2} \\ &\quad +\frac{1}{1+K^2(1-D\beta/\Delta\nu)^2}\,, \end{aligned} \tag{24}$$

$$C=\phi_3^{(3)}/2\,,$$

$$D=C^{(2)}\,,$$

$$K=\frac{\Delta\nu}{C}\,.$$

The complete profile thus appears under the simple form

$$\begin{aligned} I(\nu) &= \int_0^\infty I(\nu,\beta)H(\beta)d\beta \\ &= \frac{4}{1+K^2}+\int_0^\infty \frac{H(\beta)}{1+K^2(1+D\beta/\Delta\nu)^2}d\beta \\ &\quad +\int_0^\infty \frac{H(\beta)}{1+K^2(1-D\beta/\Delta\nu)^2}d\beta \end{aligned} \tag{25}$$

with no Doppler effect. For further analysis, it appears useful to rewrite $I(\nu)$ as

$$I(\nu)=\frac{4}{1+K^2}+I_+(\epsilon)+I_-(\epsilon)+I_+(\infty)+I_-(\infty)\,, \tag{26}$$

where

$$\begin{aligned} I_\pm &= \int_0^{\Delta\nu/D} \frac{H(\beta)}{1+K^2(1\pm D\beta/\Delta\nu)^2}d\beta \\ &\quad +\int_{\Delta\nu/D}^\infty \frac{H(\beta)}{1+K^2(1\pm D\beta/\Delta\nu)^2} \\ &\equiv I_\pm(\epsilon)+I_\pm(\infty)\,, \end{aligned} \tag{27}$$

so that

$$I_+=I_+(\epsilon)+I_+(\infty)\,,$$

$$I_-=I_-(\epsilon)+I_-(\infty)\,,$$

$$I_\pm(\epsilon)=\frac{\Delta\nu}{D}\frac{1}{(1+K^2)}\frac{A}{a}\left[\int_0^1\frac{H((\Delta\nu/D)z)dz}{(z\pm1-\sqrt{\delta})}-\int_0^1\frac{H((\Delta\nu/D)z)dz}{(z\pm1+\sqrt{\delta})}\right]$$

with

$$\begin{aligned} \delta &= 1-\frac{1}{a}=\left[\frac{i}{K}\right]^2, \\ A &= \frac{1}{2\sqrt{\delta}}=\frac{K}{2i}\,, \\ a &= \frac{K^2}{1+K^2}\,. \end{aligned} \tag{28}$$

Finally

$$\begin{aligned} I_+(\epsilon)+I_-(\epsilon) &= \frac{2}{K^2}\left\{\frac{1}{(1-\delta)}\left[\int_0^\infty H(\beta)d\beta-\int_{\Delta\nu/D}^\infty H(\beta)d\beta\right]\right. \\ &\quad \left.+\frac{(3+\delta)}{(1-\delta)^3}\left[\frac{D}{\Delta\nu}\right]^2\left[\int_0^\infty\beta^2H(\beta)d\beta-\int_{\Delta\nu/D}^\infty\beta^2H(\beta)d\beta\right]+\cdots\right\}. \end{aligned} \tag{29}$$

For large $\Delta\nu$ values ($\delta\sim0$), this becomes

$$I_+(\epsilon)+I_-(\epsilon)\sim\frac{2}{K^2}\left[\left[1-\int_{\Delta\nu/D}^\infty H(\beta)d\beta\right]+3\left[\frac{D}{\Delta\nu}\right]^2\left[\langle\beta^2\rangle-\int_{\Delta\nu/D}^\infty\beta^2H(\beta)d\beta\right]+\cdots\right] \tag{30}$$

in terms of the quadratures

$$\begin{aligned} L_1 &= \int_{\Delta\nu/D}^\infty H(\beta)d\beta \\ &= 2\left[\frac{D}{\Delta\nu}\right]^2\left[\frac{M}{N}e^{-N(\Delta\nu/D)^{1/2}}+\frac{P}{Q}e^{-Q(\Delta\nu/D)^{1/2}}\right], \end{aligned} \tag{31}$$

$$\begin{aligned} L_2 &= \int_{\Delta\nu/D}^\infty \beta^2H(\beta)d\beta \\ &= 2\frac{M}{N}e^{-N(\Delta\nu/D)^{1/2}}+2\frac{P}{Q}e^{-Q(\Delta\nu/D)^{1/2}}\,, \end{aligned} \tag{32}$$

explained with[4]

$$H(\beta)=M\frac{e^{-N\beta^{1/2}}}{\beta^{5/2}}+P\frac{e^{-Q\beta^{1/2}}}{\beta^{5/2}},\quad \beta\to\infty. \tag{33}$$

Equation (30) is then well approximated by

$$\begin{aligned} I_+(\epsilon)+I_-(\epsilon) &\sim \frac{2}{K^2}\left\{\left[1+3\left[\frac{D}{\Delta\nu}\right]^2\langle\beta^2\rangle\right]\right. \\ &\quad \left.-8\left[\frac{D}{\Delta\nu}\right]^2\left[\frac{M}{N}e^{-N(\Delta\nu/D)^{1/2}}+\frac{P}{Q}e^{-Q(\Delta\nu/D)^{1/2}}\right]\right\}. \end{aligned} \tag{34}$$

In the same vein,

$$I_+(\infty)+I_-(\infty)\sim\frac{2}{K^2}\left[\frac{D}{\Delta\nu}\right]^2\left[\frac{M}{N}e^{-N(\Delta\nu/D)^{1/2}}+\frac{P}{Q}e^{-Q(\Delta\nu/D)^{1/2}}\right]+\cdots\ . \tag{35}$$

The complete Ly α asymptotic profile (25) thus reads

$$I=\frac{4}{1+K^2}+\frac{2}{K^2}\left\{\left[1+3\left[\frac{D}{\Delta\nu}\right]^2\langle\beta^2\rangle\right]-8\left[\frac{D}{\Delta\nu}\right]^2\left[\frac{M}{N}e^{-N(\Delta\nu/D)^{1/2}}+\frac{P}{Q}e^{-Q(\Delta\nu/D)^{1/2}}\right]\right.$$
$$\left.+\frac{2}{K^2}\left[\frac{D}{\Delta\nu}\right]^2\left[\frac{M}{N}e^{-N(\Delta\nu/D)^{1/2}}+\frac{P}{Q}e^{-Q(\Delta\nu/D)^{1/2}}\right]+\cdots\right\},$$

$$\cong 2\left[\frac{C}{\Delta\nu}\right]^2\left\{\left[3+3\left[\frac{D}{\Delta\nu}\right]^2\langle\beta^2\rangle+\cdots\right]-7\left[\frac{D}{\Delta\nu}\right]^2\left[\frac{M}{N}e^{-N(\Delta\nu/D)^{1/2}}+\frac{P}{Q}e^{-Q(\Delta\nu/D)^{1/2}}\right]+\cdots\right\},\quad \frac{\Delta\nu}{C}\gg 1 \tag{36}$$

where

$$M=\frac{15}{4(2\pi)^{1/2}}\frac{(1-p)}{Z_a+p(Z_b-Z_a)}Z_a^{3/2},\quad N=\frac{2(2\pi)^{1/2}}{15}V^2Z_a^{3/2},$$

$$P=\frac{15}{4(2\pi)^{1/2}}\frac{p}{Z_a+p(Z_b-Z_a)}Z_b^{3/2},\quad Q=\frac{2(2\pi)^{1/2}}{15}V^2Z_aZ_b^{1/2},$$

$$C=5.009\,48\times10^{-21}\left\{19.288\,19-\ln\left[\frac{1}{Z_N}\left[\frac{n_e}{T_e}\right]^{1/2}\right]\right\}\frac{1}{Z_N^2}\frac{n_e}{T_e^{1/2}},$$

$$D=4.373\,66\times10^{-16}\frac{n_e^{2/3}}{Z_N}$$

in Ry, with n_e in cm^{-3} and T_e in K.

B. Ly β

Starting similarly from Eq. (21), one gets

$$I(\nu,\beta)=(2\pi Z_N)^2CS_{0z}^S$$
$$=\frac{32}{19}\left[\frac{1}{1+K^2(1+D\beta/\Delta\nu)^2}+\frac{1}{1+K^2(1-D\beta/\Delta\nu)^2}\right]+\left[\frac{1}{1+K^2(1+2D\beta/\Delta\nu)^2}+\frac{1}{1+K^2(1-2D\beta/\Delta\nu)^2}\right] \tag{37}$$

with $K=\Delta\nu/C$ and $C=\phi_3^{(3)}/2\pi$, $D=C^{(3)}$.

The final profile thus reads

$$I(\nu)=\int_0^\infty I(\nu,\beta)H(\beta)d\beta$$
$$=\frac{32}{19}\left[\int_0^\infty\frac{H(\beta)}{1+K^2(1+D\beta/\Delta\nu)^2}d\beta+\int_0^\infty\frac{H(\beta)}{1+K^2(1-D\beta/\Delta\nu)^2}d\beta\right]$$
$$+\left[\int_0^\infty\frac{H(\beta)}{1+K^2(1+2D\beta/\Delta\nu)^2}d\beta+\int_0^\infty\frac{H(\beta)}{1+K^2(1-2D\beta/\Delta\nu)^2}d\beta\right]$$
$$\equiv\frac{32}{19}(I_++I_-)+J_++J_-\ . \tag{38}$$

TABLE I. Ne X in protons ($p\simeq1$). Parameters involved in Eqs. (36) and (43).

n_e (cm^{-3})	T_e (K)	V	$\langle\beta\rangle^2$	Ly α C (Ry)	Ly α D (Ry)	Ly α $I(0)$ (Ry)	Ly β C (Ry)	Ly β D (Ry)	Ly β $I(0)$ (Ry)
2×10^{23}	1.18×10^7	0.2	24.21	8.4765×10^{-3}	1.4958×10^{-1}	3.9951	7.9159×10^{-2}	2.2437×10^{-1}	0.288 68
10^{22}	1.09×10^6	0.4	5.87	1.5418×10^{-3}	2.0301×10^{-2}	4.0196	1.5011×10^{-2}	3.0451×10^{-2}	0.731 91
2×10^{23}	2.95×10^6	0.4	5.87	1.291×10^{-2}	1.4958×10^{-1}	4.0240	1.0373×10^{-1}	2.2473×10^{-1}	0.669 95
10^{23}	1.04×10^6	0.6	2.42	1.0013×10^{-2}	9.4228×10^{-2}	4.0571	7.5767×10^{-2}	1.4134×10^{-1}	1.171 09
2×10^{23}	1.31×10^6	0.6	2.42	1.5820×10^{-2}	1.4958×10^{-1}	4.0567	1.0770×10^{-1}	2.2437×10^{-1}	1.023 48
2×10^{23}	7.37×10^5	0.8	1.28	1.7735×10^{-2}	1.4958×10^{-1}	4.1155	9.8275×10^{-2}	2.2437×10^{-1}	1.239 73
10^{24}	1.26×10^6	0.8	1.28	4.3872×10^{-2}	4.3737×10^{-1}	4.0926	5.2527×10^{-2}	6.5605×10^{-1}	0.094 27

TABLE II. Ar XVIII in protons ($p \simeq 1$). Parameters involved in Eqs. (36) and (43).

n_e (cm^{-3})	T_e (K)	V	$\langle\beta\rangle^2$	Ly α C (Ry)	Ly α D (Ry)	Ly α $I(0)$ (Ry)	Ly β C (Ry)	Ly β D (Ry)	Ly β $I(0)$ (Ry)
2×10^{23}	1.18×10^{7}	0.2	12.77	3.1453×10^{-3}	8.3058×10^{-2}	4.0038	3.1575×10^{-2}	1.2465×10^{-1}	0.183 60
10^{22}	1.09×10^{6}	0.4	2.95	5.6290×10^{-4}	1.1278×10^{-2}	4.0140	5.8080×10^{-3}	1.6917×10^{-2}	0.537 60
2×10^{23}	2.95×10^{6}	0.4	2.95	5.0427×10^{-3}	8.3098×10^{-2}	4.0183	4.6302×10^{-2}	1.2465×10^{-1}	0.602 41
10^{23}	1.04×10^{6}	0.6	1.22	3.9816×10^{-3}	5.2349×10^{-2}	4.0523	3.5415×10^{-2}	7.8523×10^{-2}	1.217 21
2×10^{23}	1.31×10^{6}	0.6	1.22	6.4707×10^{-3}	8.3098×10^{-2}	4.0540	5.4679×10^{-2}	1.2465×10^{-1}	1.177 07
2×10^{23}	7.37×10^{5}	0.8	0.65	7.5910×10^{-3}	8.3098×10^{-2}	4.1411	5.8914×10^{-2}	1.2465×10^{-1}	1.746 42
10^{24}	1.26×10^{6}	0.8	0.65	2.1637×10^{-2}	2.4298×10^{-1}	4.1375	1.2551×10^{-1}	3.6447×10^{-1}	1.227 97

$I_\pm$ have been analyzed previously [Eq. (27)], so we are left with

$$J_\pm=\int_0^{\Delta\nu/D}\frac{H(\beta)}{1+K^2(1\pm2D\beta/\Delta\nu)^2}d\beta+\int_{\Delta\nu/D}^{\infty}\frac{H(\beta)}{1+K^2(1\pm2D\beta/\Delta\nu)^2}=J_\pm(\epsilon)+J_\pm(\infty) \tag{39}$$

and

$$I(\nu)=\frac{32}{19}(I_+ + I_-)+J_+(\epsilon)+J_-(\epsilon)+J_+(\infty)+J_-(\infty)\,, \tag{40}$$

where [cf. Eq. (29)]

$$\begin{aligned}J_+(\epsilon)+J_-(\epsilon)=&\frac{2}{K^2}\left[\frac{1}{(1-\delta)}\left[\int_0^\infty H(\beta)d\beta-\int_{\Delta\nu/D}^{\infty}H(\beta)d\beta\right]\right.\\&\left.+\frac{4(3+\delta)}{(1-\delta)^3}\left[\frac{D}{\Delta\nu}\right]^2\left[\int_0^\infty\beta^2H(\beta)d\beta-\int_{\Delta\nu/D}^{\infty}\beta^2H(\beta)d\beta\right]+\cdots\right]\\&\sim\frac{2}{K^2}\left\{\left[1+4.3\left[\frac{D}{\Delta\nu}\right]^2\langle\beta^2\rangle\right]\right.\\&\left.-26\left[\frac{D}{\Delta\nu}\right]^2\left[\frac{M}{N}e^{-N(\Delta\nu/D)^{1/2}}+\frac{P}{Q}e^{-Q(\Delta\nu/D)^{1/2}}\right]+\cdots\right\},\quad\delta\sim0\end{aligned} \tag{41}$$

TABLE III. Ne X in protons. Asymptotic Ly α line ($p\simeq1$).

$\Delta\nu$	$V=0.2$, $n_e=2\times10^{23}$ cm^{-3}, $T_e=1.18\times10^{7}$ K, $I/I(0)$	$V=0.4$, $n_e=10^{22}$ cm^{-3}, $T_e=1.09\times10^{6}$ K, $I/I(0)$	$V=0.4$, $n_e=2\times10^{23}$ cm^{-3}, $T_e=2.95\times10^{6}$ K, $I/I(0)$	$V=0.6$, $n_e=2\times10^{23}$ cm^{-3}, $T_e=1.31\times10^{6}$ K, $I/I(0)$	$V=0.8$, $n_e=2\times10^{23}$ cm^{-3}, $T_e=7.37\times10^{5}$ K, $I/I(0)$	$V=0.8$, $n_e=10^{24}$ cm^{-3}, $T_e=1.26\times10^{6}$ K, $I/I(0)$
1	$1.150\,42\times10^{-4}$	$3.556\,34\times10^{-6}$	$2.695\,20\times10^{-4}$	$3.885\,76\times10^{-4}$	$4.715\,60\times10^{-4}$	$3.459\,51\times10^{-3}$
2	$2.781\,10\times10^{-5}$	$8.875\,61\times10^{-7}$	$6.373\,17\times10^{-5}$	$9.376\,02\times10^{-5}$	$1.154\,59\times10^{-4}$	$7.476\,49\times10^{-4}$
3	$1.220\,71\times10^{-5}$	$3.943\,41\times10^{-7}$	$2.795\,66\times10^{-5}$	$4.137\,35\times10^{-5}$	$5.111\,28\times10^{-5}$	$3.219\,91\times10^{-4}$
4	$6.825\,82\times10^{-6}$	$2.217\,91\times10^{-7}$	$1.564\,58\times10^{-5}$	$2.321\,28\times10^{-5}$	$2.871\,10\times10^{-5}$	$1.790\,53\times10^{-4}$
5	$4.354\,02\times10^{-6}$	$1.419\,38\times10^{-7}$	$9.988\,32\times10^{-6}$	$1.483\,83\times10^{-5}$	$1.836\,32\times10^{-5}$	$1.139\,77\times10^{-4}$
6	$3.017\,37\times10^{-6}$	$9.856\,55\times10^{-8}$	$6.926\,55\times10^{-6}$	$1.029\,76\times10^{-5}$	$1.274\,78\times10^{-5}$	$7.891\,73\times10^{-5}$
7	$2.213\,78\times10^{-6}$	$7.241\,42\times10^{-8}$	$5.084\,45\times10^{-6}$	$7.562\,58\times10^{-6}$	$9.363\,76\times10^{-6}$	$5.787\,64\times10^{-5}$
8	$1.693\,27\times10^{-6}$	$5.544\,14\times10^{-8}$	$3.890\,53\times10^{-6}$	$5.788\,61\times10^{-6}$	$7.168\,15\times10^{-6}$	$4.426\,01\times10^{-5}$
9	$1.336\,93\times10^{-6}$	$4.380\,52\times10^{-8}$	$3.072\,76\times10^{-6}$	$4.572\,90\times10^{-6}$	$5.663\,19\times10^{-6}$	$3.494\,30\times10^{-5}$
10	$1.082\,32\times10^{-6}$	$3.548\,20\times10^{-8}$	$2.488\,21\times10^{-6}$	$3.703\,58\times10^{-6}$	$4.586\,87\times10^{-6}$	$2.838\,76\times10^{-5}$
20	$2.700\,31\times10^{-7}$	$8.870\,35\times10^{-9}$	$6.214\,59\times10^{-7}$	$9.255\,20\times10^{-7}$	$1.146\,47\times10^{-6}$	$7.058\,95\times10^{-6}$
30	$1.199\,56\times10^{-7}$	$3.942\,36\times10^{-9}$	$2.761\,54\times10^{-7}$	$4.113\,11\times10^{-7}$	$5.095\,23\times10^{-7}$	$3.136\,24\times10^{-6}$
40	$6.746\,27\times10^{-8}$	$2.217\,58\times10^{-9}$	$1.553\,27\times10^{-7}$	$2.313\,56\times10^{-7}$	$2.866\,03\times10^{-7}$	$1.763\,93\times10^{-6}$
50	$4.317\,20\times10^{-8}$	$1.419\,25\times10^{-9}$	$9.940\,62\times10^{-8}$	$1.480\,66\times10^{-7}$	$1.834\,24\times10^{-7}$	$1.128\,85\times10^{-6}$
60	$2.997\,90\times10^{-8}$	$9.855\,89\times10^{-10}$	$6.903\,10\times10^{-8}$	$1.028\,23\times10^{-7}$	$1.273\,78\times10^{-7}$	$7.839\,01\times10^{-7}$
70	$2.202\,46\times10^{-8}$	$7.241\,06\times10^{-10}$	$5.071\,61\times10^{-8}$	$7.554\,33\times10^{-8}$	$9.358\,34\times10^{-8}$	$5.759\,17\times10^{-7}$
80	$1.686\,22\times10^{-8}$	$5.543\,94\times10^{-10}$	$3.882\,93\times10^{-8}$	$5.783\,76\times10^{-8}$	$7.164\,97\times10^{-8}$	$4.409\,31\times10^{-7}$
90	$1.332\,30\times10^{-8}$	$4.380\,39\times10^{-10}$	$3.067\,98\times10^{-8}$	$4.569\,88\times10^{-8}$	$5.661\,21\times10^{-8}$	$3.483\,87\times10^{-7}$
100	$1.079\,15\times10^{-8}$	$3.548\,12\times10^{-10}$	$2.485\,06\times10^{-8}$	$3.701\,60\times10^{-8}$	$4.585\,57\times10^{-8}$	$2.821\,92\times10^{-7}$

TABLE IV. Ne X in protons ($p \simeq 1$). Asymptotic Ly β line.

	$V=0.2$, $n_e=2\times10^{23}$ cm^{-3}, $T_e=1.18\times10^{7}$ K	$V=0.4$, $n_e=10^{22}$ cm^{-3}, $T_e=1.09\times10^{6}$ K	$V=0.4$, $n_e=2\times10^{23}$ cm^{-3}, $T_e=2.95\times10^{6}$ K	$V=0.6$, $n_e=2\times10^{23}$ cm^{-3}, $T_e=1.31\times10^{6}$ K	$V=0.8$, $n_e=2\times10^{23}$ cm^{-3}, $T_e=7.37\times10^{5}$ K	$V=0.8$, $n_e=10^{24}$ cm^{-3}, $T_e=1.26\times10^{6}$ K
$\Delta\nu$	$I/I(0)$	$I/I(0)$	$I/I(0)$	$I/I(0)$	$I/I(0)$	$I/I(0)$
1	2.2750×10^{-1}	1.7056×10^{-3}	1.7978×10^{-1}	1.0191×10^{-1}	5.8549×10^{-2}	6.3880×10^{-1}
2	4.1006×10^{-2}	4.1665×10^{-4}	2.8870×10^{-2}	1.8007×10^{-2}	1.1521×10^{-2}	7.2057×10^{-2}
3	1.5975×10^{-2}	1.8433×10^{-4}	1.1178×10^{-2}	7.3274×10^{-3}	4.8580×10^{-3}	2.4055×10^{-2}
4	8.4097×10^{-3}	1.0351×10^{-4}	5.9247×10^{-3}	3.9840×10^{-3}	2.6807×10^{-3}	1.1943×10^{-2}
5	5.1797×10^{-3}	6.6197×10^{-5}	3.6768×10^{-3}	2.5084×10^{-3}	1.7003×10^{-3}	7.1590×10^{-3}
6	3.5105×10^{-3}	4.5951×10^{-5}	2.5079×10^{-3}	1.7262×10^{-3}	1.1749×10^{-3}	4.7872×10^{-3}
7	2.5369×10^{-3}	3.3751×10^{-5}	1.8218×10^{-3}	1.2612×10^{-3}	8.6064×10^{-4}	3.4351×10^{-3}
8	1.9196×10^{-3}	2.5837×10^{-5}	1.3842×10^{-3}	9.6210×10^{-4}	6.5765×10^{-4}	2.5891×10^{-3}
9	1.5035×10^{-3}	2.0412×10^{-5}	1.0878×10^{-3}	7.5828×10^{-4}	5.1893×10^{-4}	2.0235×10^{-3}
10	1.2098×10^{-3}	1.6532×10^{-5}	8.7767×10^{-4}	6.1311×10^{-4}	4.1993×10^{-4}	1.6262×10^{-3}
20	2.9491×10^{-4}	4.1320×10^{-6}	2.1656×10^{-4}	1.5239×10^{-4}	1.0466×10^{-4}	3.9624×10^{-4}
30	1.3027×10^{-4}	1.8364×10^{-6}	9.6004×10^{-5}	6.7658×10^{-5}	4.6490×10^{-5}	1.7526×10^{-4}
40	7.3102×10^{-5}	1.0329×10^{-6}	5.3954×10^{-5}	3.8043×10^{-5}	2.6145×10^{-5}	9.8417×10^{-5}
50	4.6728×10^{-5}	6.6107×10^{-7}	3.4516×10^{-5}	2.4344×10^{-5}	1.6732×10^{-5}	6.2937×10^{-5}
60	3.2427×10^{-5}	4.5907×10^{-7}	2.3964×10^{-5}	1.6904×10^{-5}	1.1618×10^{-5}	4.3688×10^{-5}
70	2.3813×10^{-5}	3.3728×10^{-7}	1.7604×10^{-5}	1.2418×10^{-5}	8.5358×10^{-6}	3.2089×10^{-5}
80	1.8227×10^{-5}	2.5823×10^{-7}	1.3476×10^{-5}	9.5074×10^{-6}	6.5351×10^{-6}	2.4564×10^{-5}
90	1.4398×10^{-5}	2.0403×10^{-7}	1.0647×10^{-5}	7.5118×10^{-6}	5.1635×10^{-6}	1.9406×10^{-5}
100	1.1661×10^{-5}	1.6526×10^{-7}	8.6251×10^{-6}	6.0845×10^{-6}	4.1824×10^{-6}	1.5718×10^{-5}

and

$$J_{+}(\infty)+J_{-}(\infty)=\frac{1}{2K^2}\left[\frac{D}{\Delta\nu}\right]^2\left[\frac{M}{N}e^{-N(\Delta\nu/D)^{1/2}}+\frac{P}{Q}e^{-Q(\Delta\nu/D)^{1/2}}\right]+\cdots \,. \tag{42}$$

Equation (38) finally becomes

TABLE V. Ar XVIII in protons ($p \simeq 1$). Asymptotic Ly α line.

	$V=0.2$, $n_e=2\times10^{23}$ cm^{-3}, $T_e=1.18\times10^{7}$ K	$V=0.4$, $n_e=10^{22}$ cm^{-3}, $T_e=1.09\times10^{6}$ K	$V=0.4$, $n_e=2\times10^{23}$ cm^{-3}, $T_e=2.95\times10^{6}$ K	$V=0.6$, $n_e=2\times10^{23}$ cm^{-3}, $T_e=1.31\times10^{6}$ K	$V=0.8$, $n_e=2\times10^{23}$ cm^{-3}, $T_e=7.37\times10^{5}$ K	$V=0.8$, $n_e=10^{24}$ cm^{-3}, $T_e=1.26\times10^{6}$ K
$\Delta\nu$	$I/I(0)$	$I/I(0)$	$I/I(0)$	$I/I(0)$	$I/I(0)$	$I/I(0)$
1	1.54183×10^{-5}	4.73799×10^{-7}	3.87009×10^{-5}	6.24902×10^{-5}	8.38637×10^{-5}	7.04940×10^{-4}
2	3.75592×10^{-6}	1.18416×10^{-7}	9.54021×10^{-6}	1.55248×10^{-5}	2.08957×10^{-5}	1.71356×10^{-4}
3	1.65849×10^{-6}	5.26268×10^{-8}	4.22843×10^{-6}	6.89186×10^{-6}	9.28118×10^{-6}	7.57562×10^{-5}
4	9.30448×10^{-7}	2.96020×10^{-8}	2.37616×10^{-6}	3.87509×10^{-6}	5.21952×10^{-6}	4.25337×10^{-5}
5	5.94691×10^{-7}	1.89451×10^{-8}	1.52005×10^{-6}	2.47958×10^{-6}	3.34016×10^{-6}	2.71981×10^{-5}
6	4.12660×10^{-7}	1.31563×10^{-8}	1.05533×10^{-6}	1.72176×10^{-6}	2.31943×10^{-6}	1.88787×10^{-5}
7	3.03030×10^{-7}	9.66582×10^{-9}	7.75228×10^{-7}	1.26489×10^{-6}	1.70401×10^{-6}	1.38662×10^{-5}
8	2.31930×10^{-7}	7.40038×10^{-9}	5.93476×10^{-7}	9.68389×10^{-7}	1.30461×10^{-6}	1.06143×10^{-5}
9	1.83211×10^{-7}	5.84721×10^{-9}	4.68888×10^{-7}	7.65126×10^{-7}	1.03078×10^{-6}	8.38558×10^{-6}
10	1.48375×10^{-7}	4.73623×10^{-9}	3.79781×10^{-7}	6.19740×10^{-7}	8.34927×10^{-7}	6.79171×10^{-6}
20	3.70723×10^{-8}	1.18405×10^{-9}	9.49308×10^{-8}	1.54925×10^{-7}	2.08725×10^{-7}	1.69744×10^{-6}
30	1.64747×10^{-8}	5.26246×10^{-10}	4.21903×10^{-8}	6.88548×10^{-8}	9.27660×10^{-8}	7.54377×10^{-7}
40	9.26661×10^{-9}	2.96013×10^{-10}	2.37318×10^{-8}	3.87307×10^{-8}	5.21807×10^{-8}	4.24329×10^{-7}
50	5.93052×10^{-9}	1.89449×10^{-10}	1.51883×10^{-8}	2.47876×10^{-8}	3.33956×10^{-8}	2.71568×10^{-7}
60	4.11837×10^{-9}	1.31561×10^{-10}	1.05474×10^{-8}	1.72136×10^{-8}	2.31914×10^{-8}	1.88558×10^{-7}
70	3.02572×10^{-9}	9.66575×10^{-11}	7.74909×10^{-9}	1.26467×10^{-8}	1.70386×10^{-8}	1.38554×10^{-7}
80	2.31656×10^{-9}	7.40034×10^{-11}	5.93289×10^{-9}	9.68263×10^{-9}	1.30451×10^{-8}	1.06008×10^{-7}
90	1.83036×10^{-9}	5.84718×10^{-11}	4.68771×10^{-9}	7.65047×10^{-9}	1.03073×10^{-8}	8.38165×10^{-8}
100	1.48259×10^{-9}	4.73622×10^{-11}	3.79704×10^{-9}	6.19688×10^{-9}	8.34890×10^{-9}	6.78913×10^{-8}

TABLE VI. Ar XVIII in protons. Asymptotic Ly β line.

	$V=0.2$, $n_e=2\times10^{23}$ cm^{-3}, $T_e=1.18\times10^7$ K	$V=0.4$, $n_e=10^{22}$ cm^{-3}, $T_e=1.09\times10^6$ K	$V=0.4$, $n_e=2\times10^{23}$ cm^{-3}, $T_e=2.95\times10^6$ K	$V=0.6$, $n_e=2\times10^{23}$ cm^{-3}, $T_e=1.31\times10^6$ K	$V=0.8$, $n_e=2\times10^{23}$ cm^{-3}, $T_e=7.37\times10^5$ K	$V=0.8$, $n_e=10^{24}$ cm^{-3}, $T_e=1.26\times10^6$ K
$\Delta\nu$	$I/I(0)$	$I/I(0)$	$I/I(0)$	$I/I(0)$	$I/I(0)$	$I/I(0)$
1	4.3991×10^{-2}	3.3900×10^{-4}	2.4148×10^{-2}	1.5271×10^{-2}	1.1354×10^{-2}	1.0652×10^{-1}
2	8.5357×10^{-3}	8.4411×10^{-5}	5.1129×10^{-3}	3.5116×10^{-3}	2.7101×10^{-3}	1.9578×10^{-2}
3	3.5238×10^{-3}	3.7488×10^{-5}	2.1905×10^{-3}	1.5354×10^{-3}	1.1939×10^{-3}	8.1185×10^{-3}
4	1.9205×10^{-3}	2.1082×10^{-5}	1.2157×10^{-3}	8.5866×10^{-4}	6.6951×10^{-4}	4.4519×10^{-3}
5	1.2090×10^{-3}	1.3491×10^{-5}	7.7309×10^{-4}	5.4806×10^{-4}	4.2787×10^{-4}	2.8152×10^{-3}
6	8.3146×10^{-4}	9.3679×10^{-6}	5.3500×10^{-4}	3.8004×10^{-4}	2.9690×10^{-4}	1.9422×10^{-3}
7	6.0706×10^{-4}	6.8822×10^{-6}	3.9222×10^{-4}	2.7897×10^{-4}	2.1803×10^{-4}	1.4212×10^{-3}
8	4.6281×10^{-4}	5.2691×10^{-6}	2.9988×10^{-4}	2.1346×10^{-4}	1.6687×10^{-4}	1.0853×10^{-3}
9	3.6457×10^{-4}	4.1632×10^{-6}	2.3672×10^{-4}	1.6859×10^{-4}	1.3182×10^{-4}	8.5599×10^{-4}
10	2.9464×10^{-4}	3.3721×10^{-6}	1.9161×10^{-4}	1.3652×10^{-4}	1.0676×10^{-4}	6.9246×10^{-4}
20	7.3093×10^{-5}	8.4299×10^{-7}	4.7799×10^{-5}	3.4100×10^{-5}	2.6677×10^{-5}	1.7241×10^{-4}
30	3.2434×10^{-5}	3.7466×10^{-7}	2.1235×10^{-5}	1.5153×10^{-5}	1.1856×10^{-5}	7.6567×10^{-5}
40	1.8233×10^{-5}	2.1075×10^{-7}	1.1943×10^{-5}	8.5231×10^{-6}	6.6686×10^{-6}	4.3058×10^{-5}
50	1.1666×10^{-5}	1.3488×10^{-7}	7.6432×10^{-6}	5.4546×10^{-6}	4.2678×10^{-6}	2.7553×10^{-5}
60	8.1003×10^{-6}	9.3665×10^{-8}	5.3076×10^{-6}	3.7879×10^{-6}	2.9637×10^{-6}	1.9133×10^{-5}
70	5.9507×10^{-6}	6.8815×10^{-8}	3.8993×10^{-6}	2.7829×10^{-6}	2.1774×10^{-6}	1.4056×10^{-5}
80	4.5557×10^{-6}	5.2686×10^{-8}	2.9854×10^{-6}	2.1306×10^{-6}	1.6671×10^{-6}	1.0762×10^{-5}
90	3.5995×10^{-6}	4.1629×10^{-8}	2.3588×10^{-6}	1.6835×10^{-6}	1.3172×10^{-6}	8.5029×10^{-6}
100	2.9155×10^{-6}	3.3719×10^{-8}	1.9106×10^{-6}	1.3636×10^{-6}	1.0669×10^{-6}	6.8872×10^{-6}

$$I(\nu)\sim 2\left[\frac{C}{\Delta\nu}\right]^2\left\{\frac{51}{19}+\left[\frac{D}{\Delta\nu}\right]^2\left[\frac{324}{19}\langle\beta^2\rangle-\frac{2853}{76}\left[\frac{M}{N}e^{-N(\Delta\nu/D)^{1/2}}+\frac{P}{Q}e^{-Q(\Delta\nu/D)^{1/2}}\right]\right]\right\},$$

$$c=6.7628\times10^{-20}\left\{18.39231-\ln\left[\frac{1}{Z_N}\left[\frac{n_e}{T_e}\right]^{1/2}\right]\right\}\frac{1}{Z_N^2}\frac{n_e}{T_e^{1/2}}\mathrm{Ry} \tag{43}$$

$$D=6.56049\times10^{-16}\frac{n_e^{2/3}}{Z_N}$$

in Ry, with n_e in cm^{-3} and T_e in K.

C. Numerical results

The complete profiles (36) and (43) are respectively normalized by

$$I(0)=2\int_0^\infty\left[2+\frac{1}{1+(D\beta/C)^2}\right]H(\beta)d\beta \tag{44}$$

for Ly α and

$$I(0)=\int_0^\infty 2\left[\frac{32}{19}\left[\frac{1}{1+(D\beta/C)^2}\right]+\frac{1}{1+(2D\beta/C)^2}\right]H(\beta)d\beta \tag{45}$$

for Ly β.

As in Sec. III Ly α and β wings are worked out for Ne X and Ar XVIII with ICF plasmas in the range $10^{22}\le n_e\le10^{24}$ cm^{-3}, $7.37\times10^5\le T_e\le1.18\times10^7$ K. Particular attention is paid to the $p\cong1$ limit, where the heavy ions behave as dilute impurities. The line parameters displayed below Eqs. (36) and (43), respectively, are given numerically in Tables I and II.

The asymptotic expressions (36) and (43) are evaluated in Tables III—VI. A systematic comparison[15] between the present asymptotic $I(\nu)/I_0$ and those computed completely according to Sec. II, shows that for $\Delta\nu/D>10^2$, both calculations fall within 1% when Doppler is excluded, i.e., when

$$\Delta\nu>\begin{cases}4.37\times10^{-14}\dfrac{n_e^{2/3}}{Z_N}, & \text{Ly }\alpha\\[2ex] 6.56\times10^{-14}\dfrac{n_e^{2/3}}{Z_N}, & \text{Ly }\beta\end{cases} \tag{46}$$

with n_e in cm^{-3}.

[1]G. Bekefi, C. Deutsch, and N. Ya'akobi, in *Laser Plasmas*, edited by G. Bekefi (Wiley, New York, 1976), Chap. 13.
[2]B. Ya'akobi *et al.*, Phys. Rev. A 19, 1247 (1979).
[3]R. J. Tighe and C. F. Hooper, Jr., Phys. Rev. A 14, 1514 (1976); 17, 410 (1978).
[4]B. Held, C. Deutsch, and M.-M. Gombert, Phys. Rev. A 29, 880 (1984), preceding paper.
[5]H. R. Griem, *Spectral Line Broadening by Plasmas* (Academic, New York, 1974).
[6]C. Deutsch and G. Bekefi, Phys. Rev. A 14, 854 (1976); C. Deutsch, M. Sassi, and Gl. Coulaud, Ann. Phys. (N.Y.) 83, 1 (1974); 89, 274 (1975).
[7]M. Baranger and B. Mozer, Phys. Rev. 115, 521 (1959); 118, 626 (1960).
[8]B. Held and C. Deutsch, Phys. Rev. A 24, 540 (1981).
[9]B. Held, C. Deutsch, and M. M. Gombert, Phys. Rev. A 25, 585 (1982); J. Phys. A 15, 3845 (1982).
[10]C. F. Hooper, Jr., Phys. Rev. 149, 77 (1966); 165, 215 (1968).
[11]See, for instance, HIBALL Project Report, Kernforschungszentrum Karlsruhe, Report No. UWFDM-450, Dec. 1981 (unpublished).
[12]J. H. Nuckolls, Phys. Today 35, 25 (1982); C. Deutsch, Bull. Soc. Fr. Phys. 40, 4 (1981).
[13]R. D. Bengtson (private communication).
[14]H. E. Bethe and E. E. Salpeter, *Quantum Mechanics of One- and Two-Electron Systems* (Springer, Berlin, 1957).
[15]B. Held (private communication).